

Algebraic Reduction to Improve an Optimally Bounded Quantum State Preparation Algorithm

Giacomo Belli and Michele Amoretti

Quantum Software Laboratory, Department of Engineering and Architecture
University of Parma, 43124 Parma, Italy

Abstract

The preparation of n -qubit quantum states is a cross-cutting subroutine for many quantum algorithms, and the effort to reduce its circuit complexity is a significant challenge. In the literature, the quantum state preparation algorithm by Sun et al. is known to be optimally bounded, defining the asymptotically optimal width-depth trade-off bounds with and without ancillary qubits. In this work, a simpler algebraic decomposition is proposed to separate the preparation of the real part of the desired state from the complex one, resulting in a reduction in terms of circuit depth, total gates, and CNOT count when m ancillary qubits are available. The reduction in complexity is due to the use of a single operator Λ for each uniformly controlled gate, instead of the three in the original decomposition. Using the PennyLane library, this new algorithm for state preparation has been implemented and tested in a simulated environment for both dense and sparse quantum states, including those that are random and of physical interest. Furthermore, its performance has been compared with that of Möttönen et al.'s algorithm, which is a de facto standard for preparing quantum states in cases where no ancillary qubits are used, highlighting interesting lines of development.

keywords - *Quantum state preparation, Ancillary qubits, Fourier space, Diagonal operators*

1 Introduction

Quantum state preparation (QSP) is a fundamental subroutine in many quantum algorithms [1]. From quantum linear system solvers [2, 3, 4] to Hamiltonian simulation [5, 6, 7], from quantum chemistry [8, 9, 10, 11] to quantum machine learning [12, 13], the constant search for more efficient algorithms is still an open challenge [14, 15, 16, 17, 18, 19, 20]. The goal of a QSP algorithm is to construct a unitary operator $U \in U(2^n)$ such that $|\psi\rangle = U|0\rangle^{\otimes n}$, where $|0\rangle^{\otimes n}$ is the conventional n -qubit initial state and $|\psi\rangle = \sum_{i=0}^{2^n-1} c_i|i\rangle$ is the desired quantum state in the computational basis, normalized with respect to the l_2 -norm. The preparation can follow an exact or approximate paradigm; in the approximate version, one tries to prepare a state $|\phi\rangle$ that is ϵ -close to $|\psi\rangle$ with respect to some metric. Furthermore, the QSP algorithm can benefit from the use of ancillary registers in addition to the input registers to decrease some computational costs, such as depth, which corresponds to execution time and gate counts. Indeed, the *ancillae-based* strategy aligns with the industrial effort to scale quantum chips to ever-larger qubit counts, having to deal with intrinsically limited coherence times [21, 22]. In this industrial context, designing algorithms on larger logical registers via ancillary qubits appears to be a promising direction [23, 24, 25]. Clearly, one could try to minimize each cost measure individually, for example, by focusing only on depth. However, of particular interest is the study of the optimal space-time trade-off for quantum circuits, also with respect to hardware connectivity [26, 27].

The study of QSP began in its exact version and without ancillary qubits using the method proposed by Nielsen and Chuang [28], characterized by a depth upper bound of $\mathcal{O}(2^n)$. In the same period, Grover and Rudolph [29] proposed a *hierarchical* QSP based on layers of conditional rotations for the special case of superpositions of integrable distributions, with a depth upper bound of $\mathcal{O}(n2^n)$. Their algorithm contained what we might define today as the *embryonic form* of Uniformly Controlled Rotations (UCR) [30], even though the UCR class had not yet been formalized. In 2005, Möttönen et al. [31] proposed a 3-stage QSP that properly formalizes the UCR class, with a depth of $\mathcal{O}(2^n)$, $2^{n+2} - 4n - 4$ CNOT, and $2^{n+2} - 5$ rotations. Each UCR layer can be implemented via Gray Code [32], and its parameters can be determined via Binary Search Tree (BST) diagrams, making QSP modular [33]. Immediately after, Bergholm et al. [34], still within the framework of a general QSP, introduced and systematically analyzed the Uniformly Controlled Gate (UCG or multiplexor)

class¹ as a generalization of the UCR class. Their algorithm had an upper bound of $2^{n+1} - 2n - 2$ for the number of CNOT gates, with a depth also of order $\mathcal{O}(2^n)$.

Following the line of research on QSP, where the UCG is the key building block and no ancillary qubits are used, from 2006 to 2016, some important results structured a bridge (not only theoretical) between Gate Synthesis and QSP, where efficient general decomposition techniques (QR/CS) are combined with the modularity of UCG/UCR [30]. While Shende et al. [35] proposed a framework for synthesis pipelines, with tighter asymptotic bounds than the literature at the time and the handling of the nearest-neighbor topology, Plesch and Brukner [36] focused on minimizing the CNOT count for a general QSP with arbitrary decomposition, achieving $\frac{23}{24}2^n - 2^{\frac{n}{2}+1} + \frac{5}{3}$ for even n and $\frac{115}{96}2^n$ for odd n . Finally, Iten et al. [37] provided the framework for the systematic synthesis of isometries, within which QSP represents a special case. Their work analyzed three decompositions close to the theoretical lower bound for the number of CNOT, defining what is still an industrial benchmark². These milestones in the development of QSP clarify the link with unitary synthesis and mark the transition from the preparation of specific quantum states to the design of unitary operators, where QSP can be seen as a sub-routine for preparing columns.

The use of ancillae in the history of QSP began with Zhang et al. [38], whose algorithm can generate the target state in $\mathcal{O}(n^2)$ depth with $\mathcal{O}(2^{2n})$ ancillary qubits, but only with a limited success probability. In the same year, Rosenthal [39] tackled the topic of space-time trade-off by obtaining an algorithm with depth $\mathcal{O}(n)$ using $\mathcal{O}(n2^n)$ ancillary qubits. The *asymptotically* optimal space-time trade-off bounds were found by Sun et al. [40] in their algorithm, hereinafter referred to as SUN, with depth $\mathcal{O}(\frac{2^n}{m+n} + n \log n)$ and width $\mathcal{O}(2^n)$, where m is the number of ancillary qubits. The QSP circuit by Zhang et al. [41] of depth $\mathcal{O}(n)$ and using $\Theta(2^n)$ ancillary qubits is a special case of [40]. This line of research culminated in the work of Yuan et al. [26], which completely solves the circuit complexity with or without ancillary qubits.

This paper provides the following contributions:

1. a novel QSP algorithm that optimizes SUN in terms of depth and gate counts over the entire first range of [40, Theorem 1];
2. a simpler algebraic decomposition that splits the preparation of the real part of the desired state from the complex one and allows each UCG to be implemented with a single Λ -type constructor (instead of the 3 of the original version [40]);
3. a tighter asymptotic optimal bound for the space-time trade-off in the first range of [40, Theorem 1];
4. the implementation of the new algorithm via the PennyLane library, available on the GitHub repository [42];
5. a complete verification of the algorithm's performance through an extensive battery of tests (sparse and dense states, with complex or real coefficients, and states of interest for research) executed in a simulated environment on the HPC system of the University of Parma;
6. an explicit comparison is made in terms of depth, total gates, CNOT, and gate type with Mottonen's QSP algorithm (the standard without ancillae) and with the original version by Sun et al. (the standard for optimal complexity).

The remainder of the paper is organized as follows. In Section 2, the QSP algorithm by Sun et al. [40] is presented with its essential features, thus providing the theoretical framework and the main equations to understand its optimization. In Section 3, the new decomposition that splits the unitary QSP into two parts, one for the real part of the desired state and one for the remaining complex part, is derived, and the role of the single lambda-type constructor is discussed. The complete circuit for the $n = 2$ case is shown as an example, and Section 4 presents the results of the simulation test and the comparison with Möttönen et al.'s QSP [31] and with the implementation of the original version of Sun et al.'s QSP [43, 42]. Finally, Section 5 concludes the paper with a summary of the main results and a discussion of future work.

¹IBM Quantum, Qiskit Documentation: *UCGate class*, <https://docs.quantum.ibm.com/api/qiskit/qiskit.circuit.library.UCGate>.

²In IBM's Qiskit library, the implementation of the algorithms for state and isometry synthesis has been unified under the approach proposed by Iten, Colbeck, and Christandl [37]. In particular, the classes *StatePreparation*, *Isometry*, and *Initialize* (all within the *qiskit.circuit.library* module) invoke routines derived from this work, which thus became the reference framework for state and isometry construction in industrial quantum compilers. See IBM Quantum Documentation: <https://docs.quantum.ibm.com/api/qiskit/qiskit.circuit.library>.

2 SUN: traditional framework, diagonal operators and ancillary qubits

In [40], Sun et al. tightly characterized the depth-size complexity of the QSP problem, except for a logarithmic gap in the small parametric range $m = \left\lceil \omega \left(\frac{2^n}{n \log n} \right), o(2^n) \right\rceil$. Their algorithms, which also cover the case without ancillary qubits, allow for the construction of optimal quantum circuits where the upper and lower depth bounds coincide exactly in the two width ranges $m = \mathcal{O} \left(\frac{2^n}{n \log n} \right)$ and $m = \Omega(2^n)$. Improving on the work presented in [43], regarding the first implementation of SUN, this paper focuses on the first of the two ranges with optimal *asymptotic* complexity. In this specific domain, the traditional framework for QSP [44] can be used; it consists of a ladder structure of Uniformly Controlled Gates (UCGs) throughout the quantum register, as shown in Figure 1a. In matrix form, each UCG is a block-diagonal operator U_k belonging to $\mathbb{C}^{2^k \times 2^k}$, where each block

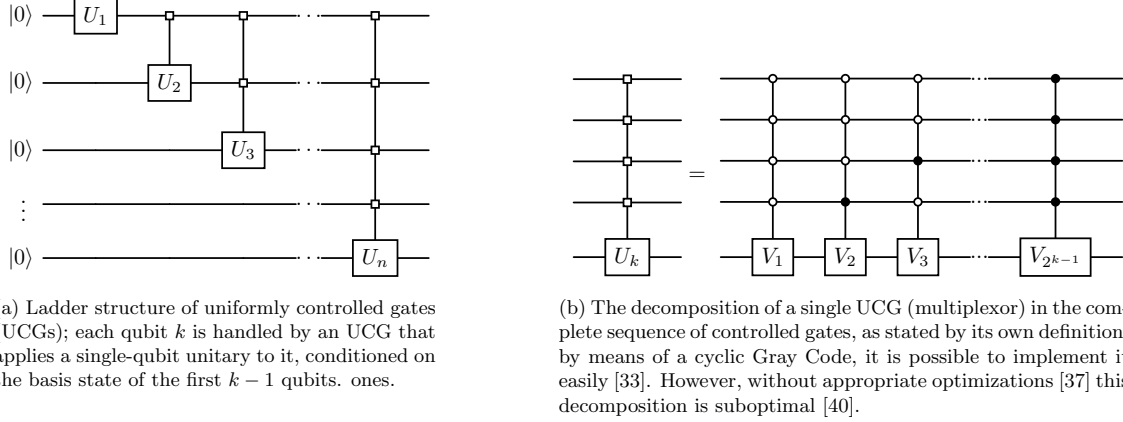


Figure 1: QSP traditional framework.

$V_j \in U(2)$ is a single-qubit gate for any $1 \leq j \leq 2^{k-1}$, in turn decomposable as $V_j = e^{i\alpha_j} R_z(\beta_j) R_y(\gamma_j) R_z(\delta_j)$ for some parameters $(\alpha, \beta, \gamma, \delta) \in \mathbb{R}$.

Actually, it is convenient to rewrite each block V_j only in terms of diagonal operators thanks to the change of gate set $R_y(\gamma_j) \equiv SH \cdot R_z(\gamma_j) \cdot HS^\dagger$. In this way, the n -qubit extension for the arbitrary UCG U_n becomes:

$$U_n = [\text{diag}(e^{i\alpha_1}, e^{i\alpha_2}, \dots, e^{i\alpha_{2^n-1}}) \otimes \mathbb{I}_1] \cdot F_n[R_z(\vec{\beta})] \cdot [\mathbb{I}_{n-1} \otimes (SH)] \cdot F_n[R_z(\vec{\gamma})] \cdot [\mathbb{I}_{n-1} \otimes (HS^\dagger)] \cdot F_n[R_z(\vec{\delta})] \quad (1)$$

where $F_n[R_z(\vec{\theta})] = \text{diag}(R_z(\theta_1), R_z(\theta_2), \dots, R_z(\theta_{2^n-1}))$. The equivalent circuit is shown in Figure 2, where the last two multi-qubit gates can be merged, being complex phase diagonal operators, thus decomposing the generic UCG with only three phase diagonal operators. It is important to note that the *central* block-diagonal operator

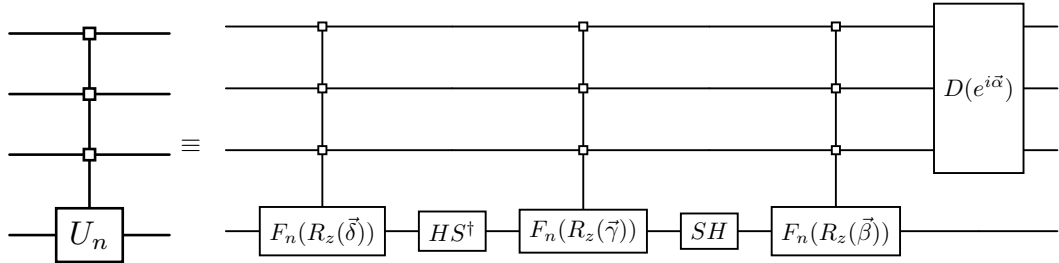


Figure 2: UCG in terms of diagonal operators $F_n(R_z)$.

$F_n(R_z(\vec{\gamma}))$ is solely responsible for preparing the real part of the desired quantum state, as the vector $\vec{\gamma}$ collects the parameters of the blocks R_y after the change of the gate set. Up to global phases³, this is already the decomposition used in [40], where diagonal Λ -type operators,

$$\Lambda_n(\vec{\theta}) = \text{diag}(1, e^{i\theta_1}, e^{i\theta_2}, \dots, e^{i\theta_{2^n-1}}) \in \mathbb{C}^{2^n \times 2^n} \quad \text{for} \quad \vec{\theta} = (\theta_1, \theta_2, \dots, \theta_{2^n-1}) \in \mathbb{R}^{2^n-1} \quad (2)$$

³A detailed mathematical proof is provided in [43].

are introduced to efficiently parallelize on an ancillary register [43]. Therefore, the arbitrary UCG U_n can be rewritten as:

$$U_n = e^{i(\alpha_1 - \beta_1)} \Lambda_n^{(1)}(\vec{\alpha}^*, \vec{\beta}^*) \cdot [\mathbb{I}_{n-1} \otimes (SH)] \cdot e^{-i\gamma_1} \Lambda_n^{(2)}(\vec{\gamma}^*) \cdot [\mathbb{I}_{n-1} \otimes (HS^\dagger)] \cdot e^{-i\delta_1} \Lambda_n^{(3)}(\vec{\delta}^*) \quad (3)$$

where $\vec{\alpha}^*, \vec{\beta}^*, \vec{\gamma}^*, \vec{\delta}^* \in \mathbb{R}^{2^n-1}$ are the vectors that group the updated Λ_n parameters after the collection of global phases. The corresponding circuit is shown in Figure 3. In the end, the traditional QSP circuit of Figure 1a

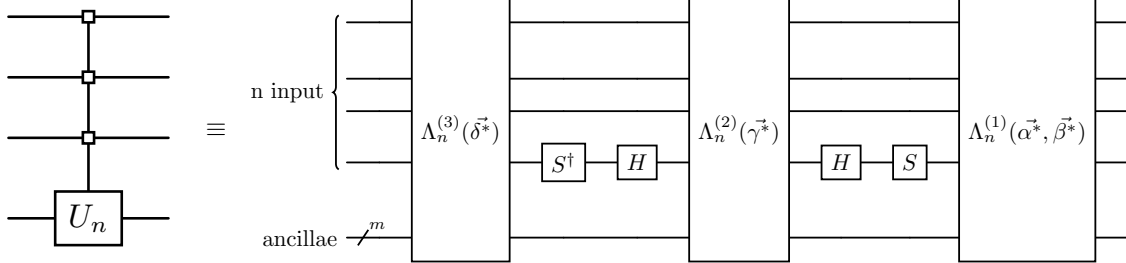


Figure 3: UCG in terms of Λ -type operators.

reduces to the concatenation of Λ_n circuits, interspersed with the two unitary operators derived from the pair of gates S and H .

In [40, Section IV], the procedure to implement any operator $\Lambda_n \in \mathbb{C}^{2^n \times 2^n}$ is discussed and proven. The equivalent quantum circuit has depth $\mathcal{O}(\log_2 m + \frac{2^n}{m})$ and width $\mathcal{O}(2^n)$, within the ancillary range $m \in [2n, \frac{2^n}{n}]$. As shown in Equation 2, matrices Λ_n perform phase shifts on each state of the computational basis, a task that can be efficiently parallelized through sums in Fourier space [43]. The key algorithm to design the Λ_n circuit has 5 stages that define the formalism for the scalable implementation; they are depicted from a high-level perspective in Figure 4. The details of their implementation, as well as the management of all parameters, are discussed in [43]. This work does not modify the basic implementation of operators Λ_n in any way, and Figure 5 shows the case for $n = 4$ as a reference example, where the 5 stages are highlighted with alternating colored bands.

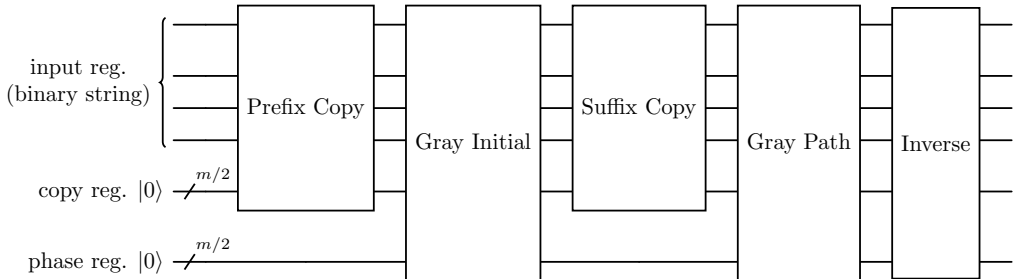


Figure 4: Λ_n quantum circuit divided into 5 sub-unitaries (stages).

2.1 Complexity analysis for SUN

This section retraces the crucial steps of the proof concerning the complexity of SUN, as presented in [40], which will be relevant in Section 3 to formally define the improvement term of its optimized version, OSUN. As stated in [40, Lemma 4], every unitary operator $\Lambda_n \in \mathbb{C}^{2^n \times 2^n}$ can be implemented by a quantum circuit of depth $\mathcal{O}(\log_2 m + \frac{2^n}{m})$, with $m \in [2n, \frac{2^n}{n}]$ ancillary qubits⁴. Thus, it is possible to define the quantity $D_\Lambda(n, m) = \log_2 m + \frac{2^n}{m}$ as the representative of the asymptotic upper-bound described in [40, Lemma 4]. In the lower bound $m = 2n$ of the parametric range, corresponding to the case implemented in [43], this quantity becomes $D_\Lambda(n, 2n) = \log_2 n + 1 + \frac{2^{n-1}}{n}$. In the case $m = 0$, the operator Λ_n can be realized with depth $\mathcal{O}(\frac{2^n}{n})$, a result stated by [40, Lemma 5].

Then, considering that the QSP circuit is built upon increasing levels of UCG (Figure 1a) and that each UCG requires three Λ -type constructors, four single-gate layers, and one global phase (Eq. 3), the overall QSP

⁴This statement has been proved in [40, Section IV].

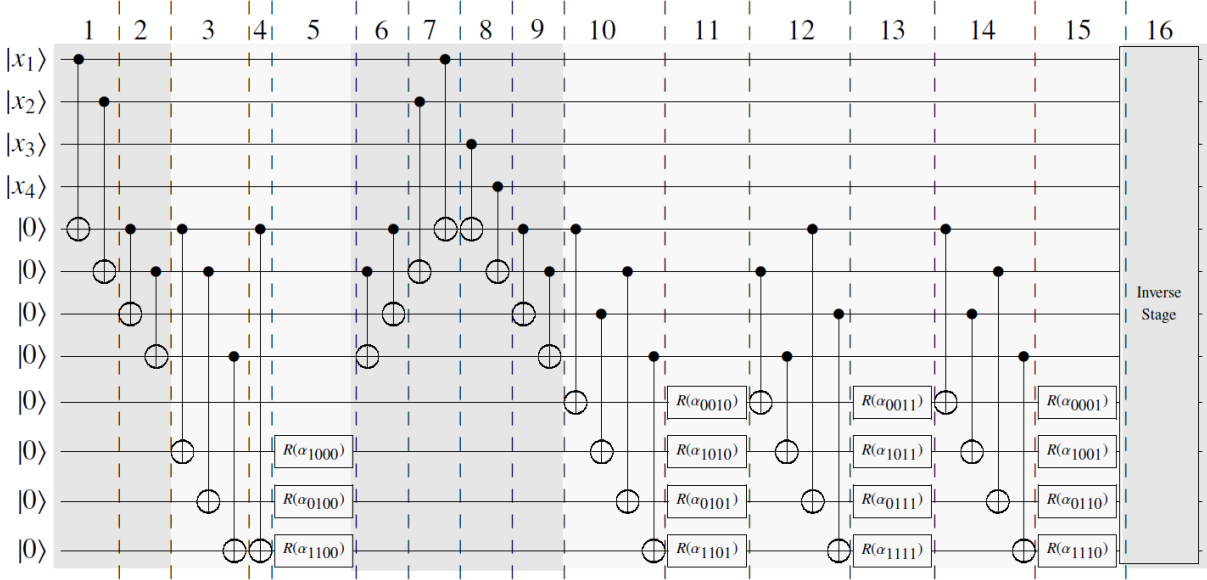


Figure 5: Quantum circuit for Λ_4 . Figure taken from [45].

circuit has depth, for $m \geq 0$:

$$D(n, m) = \sum_{k=1}^n [3D_{\Lambda}(k, m) + 4] + 1 = 3 \sum_{k=1}^n D_{\Lambda}(k, m) + 4n + 1$$

where $D_{\Lambda}(k, m)$ is the depth of each Λ -type constructor at level k , for $k \in [1, n]$ on the entire quantum register. It is shown in [40, Lemma 6] that each UCG U_n can be implemented with a circuit of depth $O(n + \frac{2^n}{n+m})$ for $m \geq 0$. For our purposes, it is useful to make explicit the construction of the latter single smooth bound. One can take the quantity $\tilde{D}(n, m) = \min\{\mathcal{O}(\log_2 m + \frac{2^n}{m}), \mathcal{O}(\frac{2^n}{n})\}$ for any $m \in [0, \frac{2^n}{n}]$ and show that $\tilde{D}(n, m) \subseteq \mathcal{O}(n + \frac{2^n}{m+n})$. Indeed, for $2n \leq m \leq \frac{2^n}{n}$, the two terms of $\mathcal{O}(\log_2 m + \frac{2^n}{m})$ are estimated, respectively,

$$\log_2 m \leq \log_2 \left(\frac{2^n}{n} \right) = n - \log_2 n = \mathcal{O}(n)$$

and

$$\frac{2^n}{m} = \frac{m+n}{m} \cdot \frac{2^n}{m+n} \leq 2 \cdot \frac{2^n}{m+n} \quad \left(\frac{m+n}{m} \leq 2 \right)$$

proving that $\mathcal{O}(\log_2 m + \frac{2^n}{m}) \subseteq \mathcal{O}(n + \frac{2^n}{n+m})$. Instead, for $0 \leq m < 2n$, it is worth noting that $\frac{2^n}{m+n} \geq \frac{2^n}{2n} = \frac{1}{2} \cdot \frac{2^n}{n}$, which shows that $\mathcal{O}(\frac{2^n}{n}) \subseteq \mathcal{O}(n + \frac{2^n}{n+m})$.

Therefore, according to the SUN procedure, a n -qubit QSP circuit with $m \geq 0$ ancillary qubits can be designed in depth $\mathcal{O}(n^2 + \frac{2^n}{n+m})$, as stated in [40, Lemma 7]. In the range $2n \leq m \leq \frac{2^n}{n^2} (\leq \frac{2^n}{n})$, previous results can be combined to derive the depth upper-bound

$$\mathcal{O} \left[\sum_{j=1}^n (\log_2 m + \frac{2^j}{m}) + n \right] = \mathcal{O} \left[(\log_2 m)n + \frac{1}{m} \sum_{j=1}^n 2^j + n \right] = \mathcal{O} \left(n^2 + \frac{2^n}{m} \right)$$

while for $m = 0$, the asymptotic complexity is $\mathcal{O} \left[\sum_{j=1}^n \frac{2^j}{j} + n \right] = \mathcal{O}(\frac{2^n}{n})$.

3 A new decomposition with a single Λ -operator for each uniformly controlled gate

As proved in [46], the traditional structure for quantum state preparation can be split into two unitaries: one devoted to the preparation of the real part of the desired state and the other to the complex component. This

separation is allowed by the conventional choice of initializing the state preparation circuits with $|0\rangle^{\otimes n}$, which in turn implies that only the first column of the total QSP unitary is relevant for preparation purposes. In this way, by concatenating the circuit block U_{mod} responsible for the preparation of the real part with a diagonal unitary D_{ph} of complex phases, a complete QSP circuit is obtained, as illustrated in Figure 6. The unitary U_{mod}

$$|0\rangle^{\otimes n} \xrightarrow{U_{mod}} |0\rangle^{\otimes n} \xrightarrow{D_{ph}} |\psi\rangle = \sum_{i=0}^{2^n-1} c_i |i\rangle$$

Figure 6: QSP structure with the separation of the real part from the complex one.

can be implemented through the traditional QSP framework [44], which is composed of Uniformly Controlled Gates (UCGs) arranged in a ladder across the entire quantum register; but, since it only needs to prepare the real part of the desired state, each UCG is a R_y -block diagonal matrix:

$$V_j = e^{i\alpha_j} R_z(\beta_j) R_y(\gamma_j) R_z(\delta_j) \in SU(2) \quad (4)$$

In order to effectively parallelize according to SUN, gate set switching is mandatory.

$$R_y(\gamma_j) \equiv SH \cdot R_z(\gamma_j) \cdot HS^\dagger \quad (5)$$

where now, contrary to the decomposition of Equation (3), each UCG U_n is encoded in a single matrix $\Lambda_n^{(2)}$, as illustrated in Figure 7. For this reason, hereafter this algorithm will be called *single- Λ ancillae-based QSP*. In analogy to Figure 2, the circuit corresponding to the unitary U_{mod} , which exploits the parallelization on the ancillary register, is represented in Figure 8. In [43, Section 2] it is shown that the ladder structure of UCG

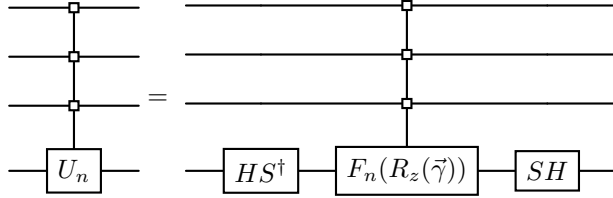


Figure 7: Reduced quantum circuit for the UCG.

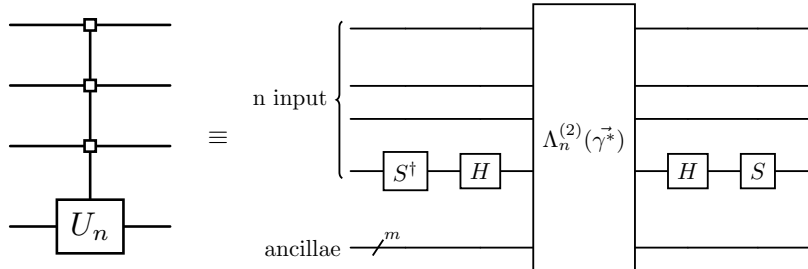


Figure 8: UCG in terms of a single Λ -type operators.

induces a simple recursive scheme on the first column of the total unitary, useful for deriving the parameters of the R_y gates according to the traditional Binary Search Tree (BST) method.

On the other hand, the diagonal unitary D_{ph} can be implemented directly via a Λ -type operator after an appropriate global phase recollection. If $|\psi\rangle = \sum_{k=0}^{2^n-1} c_k |e^{i\phi_k} k\rangle$, the complex phases $e^{i(\phi_k - \phi_0)}$ will be the diagonal entries of D_{ph} for $0 \leq k \leq 2^n - 1$, where $e^{i\phi_0}$ is the global phase.

Ultimately, according to the new decomposition summarized in the 2-unitary block structure of Figure 6, the overall reduced-depth quantum circuit for the preparation of a 2-qubit (4-ancilla) arbitrary state is depicted in Figure 9.

3.1 Complexity analysis for OSUN

The optimized version of SUN described in Section 3, hereafter referred to as OSUN, uses only one (instead of three) circuit block Λ_k for each UCG dedicated to the real part of the desired state, and a final block Λ_n

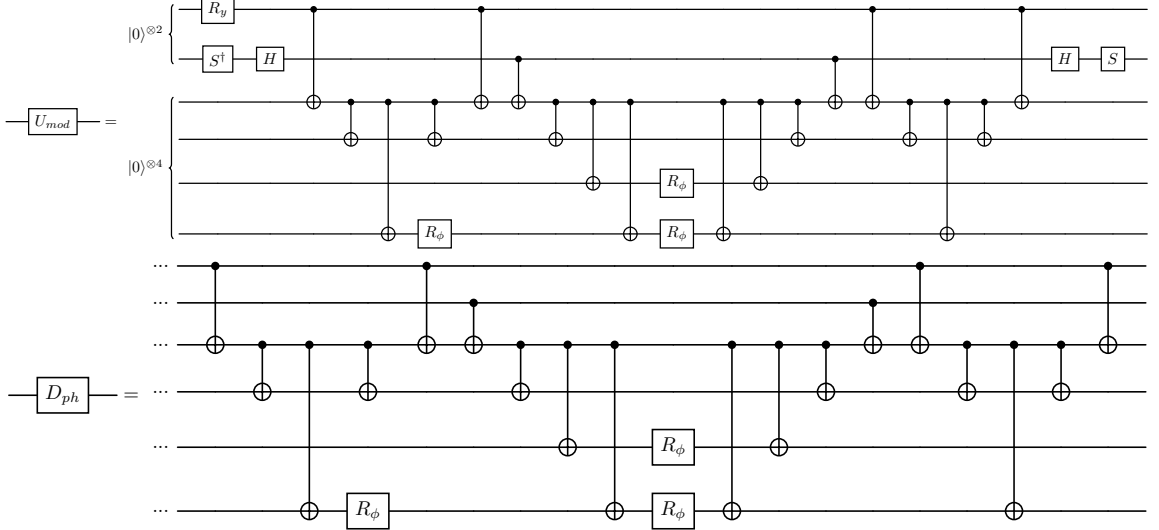


Figure 9: QSP circuit for $n = 2$ divided into the two unitary blocks U_{mod} and D_{ph} .

for the imaginary part, in the parametric range $2n \leq m \leq \frac{2^n}{n}$. Therefore, the whole n -qubit QSP circuit has depth $D(n, m) = \sum_{k=1}^n [D_\Lambda(k, m) + 4] + 1 + D_\Lambda(n, m)$, which essentially leads to the same complexity: the improvement term is hidden in the constant factors of the two main contributions. For this reason, reproducing the complexity analysis of Section 2 using a model with *explicit constants* will allow us to formally define the improvement.

SUN complexity model with explicit constant

In the parametric range $2n \leq m \leq \frac{2^n}{n}$, each operator Λ_j has depth $D_\Lambda^{anc}(j, m) \leq a \log_2 m + b \frac{2^j}{m}$ for any real numbers $a, b > 0$ and $j \in [1, n]$. In each level j , the UCG U_j also counts four single-qubit layers and one global phase, for a total cost indicated below as c . When no ancillary qubits are available, each operator Λ_j has depth $D_\Lambda^{no-anc}(j) \leq d \frac{2^j}{j}$, for any real $d > 0$. Therefore, the construction of a single smooth bound $m \geq 0$ for the depth of each UCG U_j leads one to consider:

$$D_j^{case}(m) \leq 3D_\Lambda^{case}(j, m) + c = \begin{cases} 3a \log_2 m + 3b \frac{2^j}{m} + c & \text{case} = anc \\ 3d \frac{2^j}{j} + c & \text{case} = no - anc \end{cases}$$

In the following, it is shown that there exists a real $k > 0$ such that $D_j^{case}(m) \leq k(n + \frac{2^n}{n+m})$ for $m \geq 0$, considering two cases:

a) in the range $2n \leq m \leq \frac{2^n}{n}$, $\log_2 m \leq \log_2(\frac{2^n}{n}) = n - \log_2 n \leq n$, thus $3a \log_2 m \leq 3an$. Instead, $\frac{2^j}{m} = \frac{m+n}{m} \cdot \frac{2^j}{m+n} \leq \frac{3}{2} \frac{2^j}{m+n}$, thus $3b \frac{2^j}{m} \leq \frac{9}{2} b \frac{2^j}{m+n}$. Therefore,

$$D_j^{anc}(m) \leq 3an + \frac{9b}{2} \frac{2^j}{m+n} + c \leq k_1 \left(n + \frac{2^n}{m+n} \right)$$

for $k_1 \geq \max\{3a, \frac{9b}{2}, c\}$.

b) in the range $0 \leq m < 2n$, it is simple to see that $\frac{2^j}{j+m} \in (\frac{2^j}{2n+j}, \frac{2^j}{j}]$, since $j \leq j+m < 2n+j$. Then $\frac{2^j}{j} \leq (\frac{2n}{j} + 1) \frac{2^j}{j+m}$ and

$$D_j^{no-anc}(m) \leq 3d \frac{2^j}{j} + c \leq 3d \left(\frac{2n}{j} + 1 \right) \frac{2^j}{j+m} + c \leq 3d \left(\frac{2n}{j} + 1 \right) \left(n + \frac{2^n}{n+m} \right) + c \leq k_2 \left(n + \frac{2^n}{n+m} \right)$$

for $k_2 \geq \max \left\{ 3d \left(\frac{2n}{j} + 1 \right), c \right\}$.

As a consequence, taking $k = \max\{k_1, k_2\}$, $D_j^{case}(m) \in \mathcal{O}(n + \frac{2^n}{n+m})$.

The total depth of the circuit can be computed, respectively, in the range $2n \leq m \leq \frac{2^n}{n}$ by

$$D(n, m)^{anc} = \sum_{j=1}^n D_j^{anc}(m) \leq 3an \log m + \frac{3b}{m}(2^{n+1} - 2) + cn = \mathcal{O}(n^2) + \mathcal{O}\left(\frac{2^n}{m}\right) = \mathcal{O}\left(n^2 + \frac{2^n}{m}\right) \quad (6)$$

and in the range $0 \leq m < 2n$ by

$$D(n)^{no-anc} = \sum_{j=1}^n D_j^{no-anc} \leq 3dS_n + cn$$

where $S_n := \sum_{j=1}^n \frac{2^j}{j} = \sum_{j=1}^{\lfloor n/2 \rfloor} \frac{2^j}{j} + \sum_{\lfloor n/2 \rfloor + 1}^n \frac{2^j}{j}$. In the latter expression,

$$\sum_{j=1}^{\lfloor n/2 \rfloor} \frac{2^j}{j} \leq \sum_{j=1}^{\lfloor n/2 \rfloor} 2^j \leq 2^{n/2+1}$$

while

$$\sum_{\lfloor n/2 \rfloor + 1}^n \frac{2^j}{j} \leq \frac{2}{n} \sum_{\lfloor n/2 \rfloor + 1}^n 2^j \leq \frac{2}{n} 2^{n+1}$$

so that $S_n \leq 2^{n/2+1} + \frac{4}{n} 2^n \leq k_3 \frac{2^n}{n}$ and

$$D(n)^{no-anc} \leq 3dk_3 \frac{2^n}{n} + cn = \mathcal{O}\left(\frac{2^n}{n}\right) \quad (7)$$

Consistency at the edge $m = 2n$ is ensured by

$$D(n, 2n)^{anc} = 3an \log(2n) + \frac{3b}{2n}(2^{n+1} - 2) + cn \approx 3an \log n + \frac{3b}{n} 2^n + \mathcal{O}(n) = \mathcal{O}\left(\frac{2^n}{n}\right)$$

meaning that the two regimes connect without any jumps.

OSUN complexity model with explicit constant

Based on the algebraic reduction described in Section 3, valid in the parametric range $m \in [2n, \frac{2^n}{n}]$, the optimized version OSUN has a ladder structure of R_y -based UCGs starting from level $j = 2$. This is because level $j = 1$ only has one uncontrolled gate R_y (refer to Figure 9 as an example), which is possible due to the hypothesis of preparing the real part of the desired state separately from the complex part. This simplification has the following consequences:

- level $j = 1$ has a constant depth $c_0 = 2$;
- for each level $j \in [2, n]$, there are two single-gate layers, which we denote as cost $c_1 = 2$;
- for each level $j \in [2, n]$, there is one Λ -type constructor for the real part, plus another one for $j = n$ regarding the imaginary part of the desired state;
- c_3 is the cost of the global phase.

Then, based on the new decomposition summarized by Figure 8, the total depth can be evaluated as

$$D_{opt}^{anc}(n, m) = c_0 + \sum_{j=2}^n [D_{\Lambda}^{anc}(j, m) + c_1] + D_{\Lambda}^{anc}(n, m) + c_3$$

where $D_{\Lambda}^{anc}(j, m) \leq a \log m + b \frac{2^j}{m}$ for real $a, b > 0$, as before. Considering that $\sum_{j=2}^n b \frac{2^j}{m} = \frac{b}{m}(2^{n+1} - 4)$,

$$D_{opt}^{anc}(n, m) \leq an \log m + \frac{b}{m}(3 \cdot 2^n - 4) + c_1 n + \mathcal{O}(1) \quad (8)$$

From a quick comparison with Equation 6, it is clear that term $n \log m$ shows a factor of 3 improvement, while term $\frac{2^n}{m}$ shows a factor of 2 improvement; on the contrary, the linear terms are similar and absorbed by $\mathcal{O}(n^2)$ in the global bound. It is also clear that the algebraic reduction has not changed the complexity class: on the

range $2n \leq m \leq \frac{2^n}{n}$, $an \log m \leq an^2$, so that $D_{opt}^{anc}(n, m) \in \mathcal{O}(n^2 + \frac{2^n}{m})$. In conclusion, the new construction has the same asymptotic complexity but systematically lowers the prefactors of the two dominant contributions (linear-logarithmic and exponential).

For completeness, the analysis of OSUN in the range $0 \leq m < 2n$ is reported below. Applying the same assumptions as in the previous range, the total depth is given by

$$D_{opt}^{no-anc}(n) = c_0 + \sum_{j=2}^n [D_{\Lambda}^{no-anc}(j, m) + c_1] + D_{\Lambda}^{no-anc}(n, m) + c_3$$

where now $D_{\Lambda}^{no-anc}(j) \leq d \frac{2^j}{j}$, for real $d > 0$. Remembering that $S_n := \sum_{j=1}^n \frac{2^j}{j}$, it is worth that $\sum_{j=2}^n \frac{2^j}{j} \leq S_n \leq k \frac{2^n}{n}$, so that

$$D_{opt}^{no-anc}(n) \leq d(k+1) \frac{2^n}{n} + cn + \mathcal{O}(1) = \mathcal{O}\left(\frac{2^n}{n}\right) \quad (9)$$

The comparison with Equation 7 also shows, in this case, the reduction of the prefactor of the dominant term.

4 Simulations and Results

The *single- Λ ancillae-based* QSP algorithm has been tested using the PennyLane simulator [47] on a Linux machine equipped with an AMD EPYC 7282 CPU and 256 GB of RAM. First, the preparation of some quantum states of interest for research was verified: the four Bell states for 2 qubits, as well as the GHZ, W, and Dicke states for 3 and 4 qubits. The results are reported in Table 1, where the columns “Time Classical” and “Time Quantum” indicate, respectively, the time for determining the parameters (classical subroutine) and the time for the execution of the quantum circuit in a simulated environment. Depending on their amplitudes, not all states require the general circuit of the complex case (see Figure 6 for the general structure and Figure 9 as an example for 2 qubits): states with positive real coefficients can be prepared with a reduced circuit, which corresponds to the only U_{mod} unitary of Figure 6.

Simulation results for specific quantum states								
n	Target State	Avg Fidelity $\sigma^2 \leq 10^{-32}$	Avg Trace Distance $\sigma^2 = 0.0$	Depth	Total gates	CNOT	Avg Time Classical (s)	Avg Time Quantum (s)
2	Bell Φ_+	$1 - 2 \times 10^{-16}$	2.78×10^{-16}	20	26	18	1.41×10^{-3}	3.54×10^{-2}
	Bell Φ_-	$1 - 2 \times 10^{-16}$	2.78×10^{-16}	39	47	36	7.11×10^{-3}	4.20×10^{-2}
	Bell Ψ_+	$1 - 2 \times 10^{-16}$	2.78×10^{-16}	20	26	18	1.17×10^{-3}	3.77×10^{-2}
	Bell Ψ_-	$1 - 2 \times 10^{-16}$	2.78×10^{-16}	39	47	36	6.89×10^{-3}	2.75×10^{-2}
3	GHZ	$1 - 6 \times 10^{-16}$	4.16×10^{-16}	43	67	48	4.13×10^{-3}	4.26×10^{-2}
	W	$1 - 6 \times 10^{-16}$	3.05×10^{-16}	43	67	48	2.81×10^{-3}	4.84×10^{-2}
	Dicke	$1 - 6 \times 10^{-16}$	3.05×10^{-16}	43	67	48	2.89×10^{-3}	5.81×10^{-2}
4	GHZ	$1 - 9 \times 10^{-16}$	7.49×10^{-16}	74	142	104	8.65×10^{-3}	7.30×10^{-2}
	W	$1 - 9 \times 10^{-16}$	5.83×10^{-16}	74	142	104	6.70×10^{-3}	8.27×10^{-2}
	Dicke	$1 - 9 \times 10^{-16}$	5.27×10^{-16}	74	142	104	6.74×10^{-3}	7.60×10^{-2}

Table 1: Preparation of well-known quantum states. The results refer to a sample of 20 states.

In a second step, the effectiveness of the algorithm has been verified in the preparation of random quantum states, both dense and sparse, with real positive, real negative, or complex coefficients, from 2 to 5 qubits. The results are reported in Tables 2, 3 and 4.

Finally, not noticing any substantial differences between the previously analyzed categories, the novel QSP algorithm has been tested from 6 to 10 qubits for random states, both dense and sparse, with only complex coefficients. The results are reported in Table 5.

The QSP algorithm based on the new algebraic decomposition that uses a single Λ -type constructor for each UCG has been compared with the well-known algorithm by Möttönen et al. [44], here denoted as MOTT, which is considered a reference standard for QSP without ancillary qubits. The comparison is meaningful because both algorithms are based on the traditional QSP structure defined by the UCG ladder sequence (Figure 1a). Some metrics are shown in Figures 10, 11, 12, and 13. A comparison with the developments that followed the algorithm of Möttönen et al., such as those proposed by Bergholm [34], by Plesch and Brukner [36], or with the generalizations introduced by Iten [37], has not been covered in this work and will be the heart of a

Simulation results for random states with complex amplitudes							
n	Type of state	Avg Fidelity $\sigma^2 \in [10^{-32}, 10^{-31}]$	Avg Trace Distance $\sigma^2 \in [10^{-33}, 10^{-32}]$	Depth	CNOT gates	Avg Time Classical (s)	Avg Time Quantum (s)
2	dense	$1 - 2 \times 10^{-16}$	2.43×10^{-16}	39	36	7.88×10^{-3}	6.11×10^{-2}
	sparse	$1 - 3 \times 10^{-16}$	2.58×10^{-16}			1.06×10^{-2}	3.87×10^{-2}
3	dense	$1 - 6 \times 10^{-16}$	3.79×10^{-16}	66	78	7.21×10^{-3}	8.90×10^{-2}
	sparse	$1 - 3 \times 10^{-16}$	3.07×10^{-16}			3.69×10^{-3}	5.92×10^{-2}
4	dense	$1 - 9 \times 10^{-16}$	5.71×10^{-16}	105	160	8.46×10^{-3}	8.91×10^{-2}
	sparse	$1 - 9 \times 10^{-16}$	5.48×10^{-16}			8.56×10^{-3}	8.64×10^{-2}
5	dense	$1 - 2 \times 10^{-15}$	7.48×10^{-16}	166	276	6.30×10^{-2}	1.55×10^{-1}
	sparse	$1 - 2 \times 10^{-15}$	7.47×10^{-16}			5.05×10^{-2}	1.39×10^{-1}

Table 2: Preparation of random quantum states with complex coefficients. The results refer to a sample of 20 states.

Simulation results for random states with real positive amplitudes							
n	Type of state	Avg Fidelity $\sigma^2 \in [10^{-32}, 10^{-31}]$	Avg Trace Distance $\sigma^2 \in [10^{-33}, 10^{-30}]$	Depth	CNOT gates	Avg Time Classical (s)	Avg Time Quantum (s)
2	dense	$1 - 3 \times 10^{-16}$	2.61×10^{-16}	20	18	1.17×10^{-3}	5.47×10^{-2}
	sparse	$1 - 3 \times 10^{-16}$	2.23×10^{-16}			1.13×10^{-3}	5.74×10^{-2}
3	dense	$1 - 6 \times 10^{-16}$	3.58×10^{-16}	43	48	2.50×10^{-3}	6.19×10^{-2}
	sparse	$1 - 6 \times 10^{-16}$	5.26×10^{-16}			2.37×10^{-3}	7.27×10^{-2}
4	dense	$1 - 7 \times 10^{-16}$	8.98×10^{-16}	74	104	6.65×10^{-3}	9.13×10^{-2}
	sparse	$1 - 7 \times 10^{-16}$	5.33×10^{-16}			6.62×10^{-3}	8.76×10^{-2}
5	dense	$1 - 2 \times 10^{-15}$	7.96×10^{-16}	120	190	6.24×10^{-2}	1.47×10^{-1}
	sparse	$1 - 2 \times 10^{-15}$	6.16×10^{-16}			7.71×10^{-2}	1.32×10^{-1}

Table 3: Preparation of random quantum states with real positive coefficients. The results refer to a sample of 20 states.

Simulation results for random states with real negative amplitudes							
n	Type of state	Avg Fidelity $\sigma^2 \in [10^{-32}, 10^{-31}]$	Avg Trace Distance $\sigma^2 \in [10^{-33}, 10^{-29}]$	Depth	CNOT gates	Avg Time Classical (s)	Avg Time Quantum (s)
2	dense	$1 - 2 \times 10^{-16}$	2.17×10^{-16}	39	36	6.37×10^{-3}	3.14×10^{-2}
	sparse	$1 - 2 \times 10^{-16}$	2.64×10^{-16}			8.82×10^{-3}	3.22×10^{-2}
3	dense	$1 - 7 \times 10^{-16}$	3.74×10^{-16}	66	78	1.23×10^{-2}	5.44×10^{-2}
	sparse	$1 - 7 \times 10^{-16}$	5.31×10^{-16}			6.42×10^{-3}	4.66×10^{-2}
4	dense	$1 - 2 \times 10^{-15}$	6.12×10^{-16}	105	160	1.42×10^{-2}	8.13×10^{-2}
	sparse	$1 - 2 \times 10^{-15}$	6.25×10^{-16}			1.41×10^{-2}	8.51×10^{-2}
5	dense	$1 - 2 \times 10^{-15}$	1.70×10^{-15}	166	276	6.32×10^{-2}	1.54×10^{-1}
	sparse	$1 - 2 \times 10^{-15}$	8.88×10^{-16}			5.08×10^{-2}	1.69×10^{-1}

Table 4: Preparation of random quantum states with real negative coefficients. The results refer to a sample of 20 states.

Simulation results for random states with complex amplitudes							
n	Type of state	Avg Fidelity $\sigma^2 \in [10^{-31}, 10^{-30}]$	Avg Trace Distance $\sigma^2 \in [10^{-32}, 10^{-31}]$	Depth	CNOT gates	Avg Time Classical (s)	Avg Time Quantum (s)
6	dense	$1 - 2 \times 10^{-15}$	8.22×10^{-16}	246	510	1.43×10^{-1}	4.23×10^{-1}
	sparse	$1 - 3 \times 10^{-15}$	8.99×10^{-16}			1.62×10^{-1}	4.30×10^{-1}
7	dense	$1 - 3 \times 10^{-15}$	1.11×10^{-15}	427	930	3.40×10^{-1}	2.22
	sparse	$1 - 3 \times 10^{-15}$	1.21×10^{-15}			3.88×10^{-1}	2.23
8	dense	$1 - 3 \times 10^{-15}$	1.32×10^{-15}	647	1748	9.74×10^{-1}	4.23×10^2
	sparse	$1 - 3 \times 10^{-15}$	1.11×10^{-15}			8.98×10^{-1}	4.53×10^2
9	dense	$1 - 3 \times 10^{-15}$	1.66×10^{-15}	1046	3354	3.70	2.63×10^3
	sparse	$1 - 3 \times 10^{-15}$	1.30×10^{-15}			3.59	2.58×10^3
10	dense	$1 - 3 \times 10^{-15}$	1.55×10^{-15}	1871	6486	14.4	1.97×10^4
	sparse	$1 - 3 \times 10^{-15}$	1.52×10^{-15}			14.9	2.06×10^4

Table 5: Preparation of random quantum states with complex coefficients. The results refer to a sample of 20 states.

more systematic future benchmarking⁵. The new decomposition proposed in this work, compared to MOTT, shows a significant reduction in depth already at the lower end of the first range of [40, Theorem 1], where the auxiliary register grows only polynomially ($m = 2n$). Other points in Sun et al.’s parametric domain may show even greater reductions in light of this new decomposition. Therefore, comparison with Möttönen’s current optimizations should be made once the optimal time-space trade-off is defined.

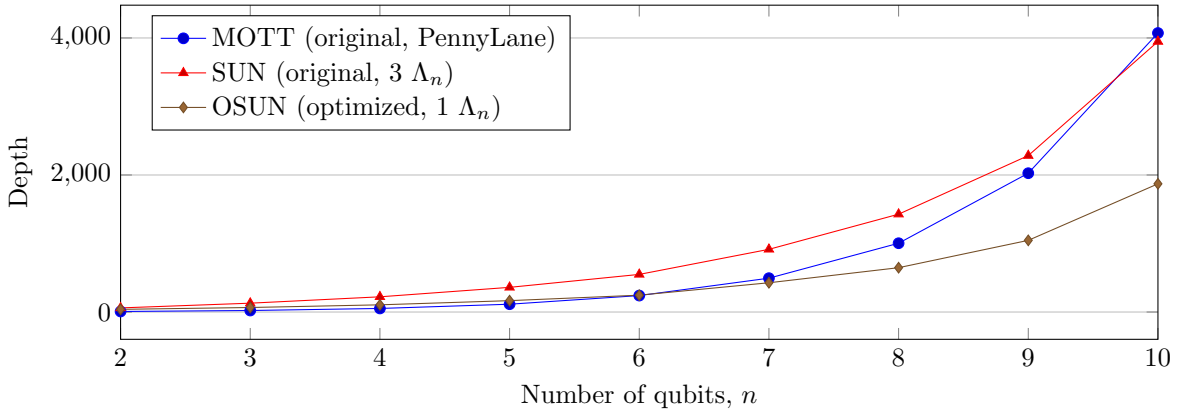


Figure 10: Depth vs n

5 Conclusions

In the traditional QSP framework based on successive UCG levels, the hypothesis of preparing the real part of the desired state separately from the complex part leads to an algebraic simplification. In fact, if the UCG ladder structure is entrusted with the task of preparing only the real moduli of each component of the target state, each UCG can be built with only R_y -blocks, which, in turn, can be implemented in terms of R_z , H , and S gates. This reduction has a precise consequence for the QSP algorithm SUN, known in the literature for defining the optimal asymptotic space-time trade-off: for $2n \leq m \leq \frac{2^n}{n}$ ancillary qubits, each UCG can be implemented with one lambda operator (instead of 3), leading to systematic depth improvements. The complex part of the desired state is instead prepared with a single, maximum-dimensional lambda operator at the end of the UCG scheme. This new QSP algorithm, denoted as OSUN, does not change the complexity of SUN but improves the prefactors of the dominant terms, specifically by a factor of 3 in the linear term and by a factor of 2 in the exponential term. It is important to note that this algebraic reduction applies to the entire first parametric range of [40, Theorem 1], so future extensions of the algorithm to points in the domain where the ancillary register grows exponentially would benefit from the same optimization.

⁵The authors are aware of the recent result published by Carvalho et al. [48] on the UCG class, which will also be compared

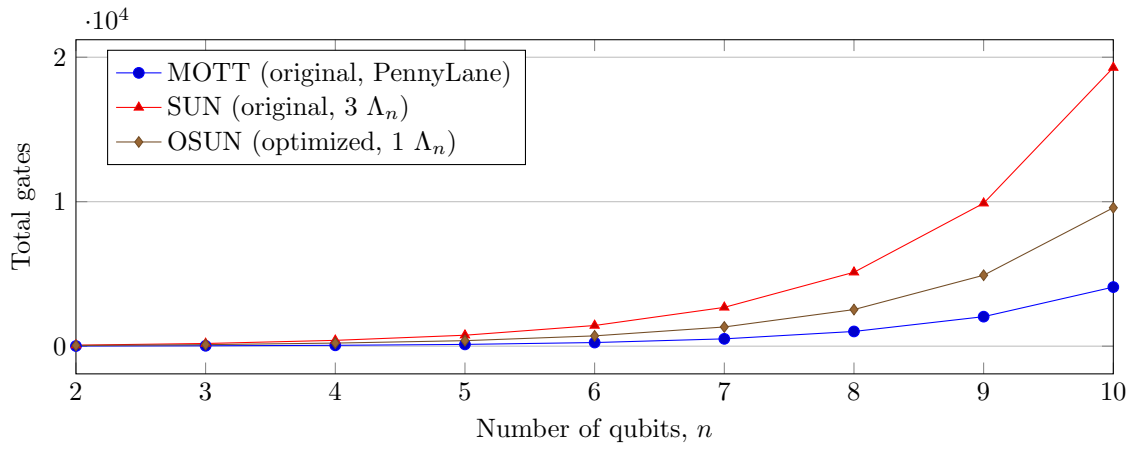


Figure 11: Total gates vs n

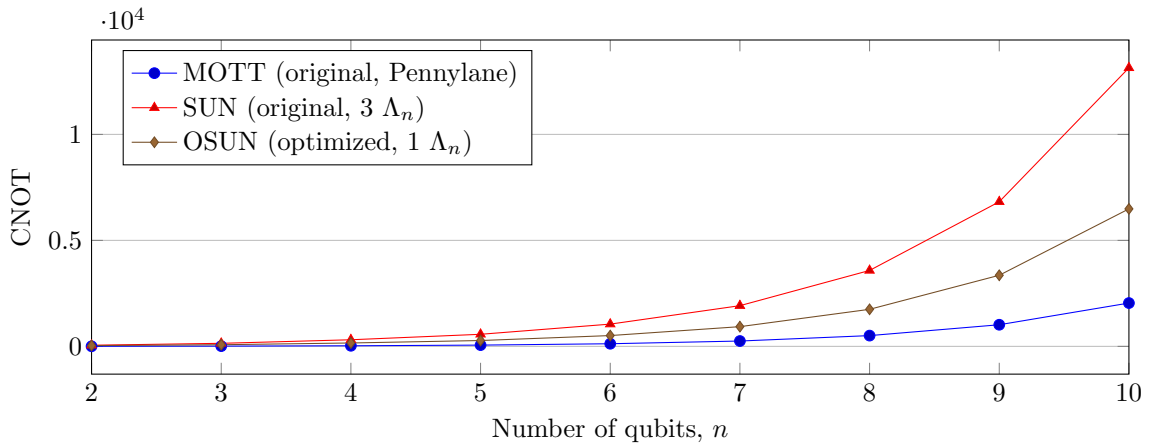


Figure 12: CNOT vs n

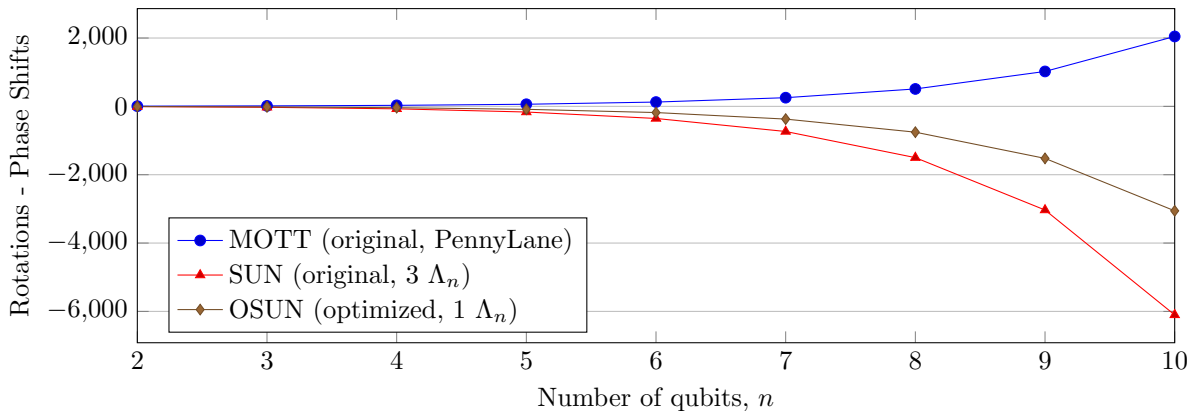


Figure 13: Difference between rotations and phase shifts vs n

The OSUN algorithm has been implemented with the PennyLane library, and the code is available on GitHub [42]. The effectiveness of the algorithm has been verified in simulations involving up to 10 qubits for various types of target states. For each case, metrics such as depth, number of CNOTs, classical precomputation time, and quantum circuit simulation time have been reported. Furthermore, the new algorithm OSUN has been compared with the original version SUN and with the well-known Möttönen algorithm MOTT, which is an important reference as it is based on the same UCG scheme but does not use ancillary qubits. The results clearly show that OSUN has a shallower depth starting from 6 qubits, with a smoother growth curve compared to the original version, thanks to the optimization of the prefactors of the dominant terms. Regarding the total number of gates (and the number of CNOTs), OSUN does not improve upon MOTT. Note, however, that the gate set of CNOTs and rotations of MOTT is converted to a gate set of CNOTs and phase shifts in OSUN. Future developments could concern the extension of OSUN to other points in the parametric domain to better exploit the depth reductions afforded by the ancillae parallelization and systematic comparisons with the most recent implementations of the UCG class. Other topics to consider are qubit connectivity and how it affects performance on real hardware, or to what extent a translation in the Clifford+T gate set could affect the complexity.

Acknowledgments

Giacomo Belli and Michele Moretti acknowledge financial support from the European Union - NextGenerationEU, PNRR MUR project PE0000023-NQSTI. This research benefits from the High Performance Computing facility of the University of Parma, Italy (HPC.unipr.it).

References

- [1] Jason Iaconis, Sonika Johri, and Elton Yechao Zhu. Quantum state preparation of normal distributions using matrix product states. *npj Quantum Information*, 10(1):15, 2024.
- [2] Aram W Harrow, Avinatan Hassidim, and Seth Lloyd. Quantum algorithm for linear systems of equations. *Physical review letters*, 103(15):150502, 2009.
- [3] Mauro ES Morales, Lirandë Pira, Philipp Schleich, Kelvin Koor, Pedro Costa, Dong An, Alán Aspuru-Guzik, Lin Lin, Patrick Rebentrost, and Dominic W Berry. Quantum linear system solvers: A survey of algorithms and applications. *arXiv preprint arXiv:2411.02522*, 2024.
- [4] Carlos Bravo-Prieto, Ryan LaRose, Marco Cerezo, Yigit Subasi, Lukasz Cincio, and Patrick J Coles. Variational quantum linear solver. *Quantum*, 7:1188, 2023.
- [5] Dominic W Berry, Mária Kieferová, Artur Scherer, Yuval R Sanders, Guang Hao Low, Nathan Wiebe, Craig Gidney, and Ryan Babbush. Improved techniques for preparing eigenstates of fermionic hamiltonians. *npj Quantum Information*, 4(1):22, 2018.
- [6] Guang Hao Low and Isaac L Chuang. Hamiltonian simulation by qubitization. *Quantum*, 3:163, 2019.
- [7] Ryan Babbush, Craig Gidney, Dominic W Berry, Nathan Wiebe, Jarrod McClean, Alexandru Paler, Austin Fowler, and Hartmut Neven. Encoding electronic spectra in quantum circuits with linear t complexity. *Physical Review X*, 8(4):041015, 2018.
- [8] Sam McArdle, Suguru Endo, Alán Aspuru-Guzik, Simon C Benjamin, and Xiao Yuan. Quantum computational chemistry. *Reviews of Modern Physics*, 92(1):015003, 2020.
- [9] Stepan Fomichev, Kasra Hejazi, Modjtaba Shokrian Zini, Matthew Kiser, Joana Fraxanet, Pablo Antonio Moreno Casares, Alain Delgado, Joonsuk Huh, Arne-Christian Voigt, Jonathan E Mueller, et al. Initial state preparation for quantum chemistry on quantum computers. *PRX Quantum*, 5(4):040339, 2024.
- [10] Guoming Wang, Sukin Sim, and Peter D Johnson. State preparation boosters for early fault-tolerant quantum computation. *Quantum*, 6:829, 2022.
- [11] Dominic W Berry, Yu Tong, Tanuj Khattar, Alec White, Tae In Kim, Guang Hao Low, Sergio Boixo, Zhiyan Ding, Lin Lin, Seunghoon Lee, et al. Rapid initial-state preparation for the quantum simulation of strongly correlated molecules. *PRX Quantum*, 6(2):020327, 2025.

[12] Minati Rath and Hema Date. Quantum data encoding: A comparative analysis of classical-to-quantum mapping techniques and their impact on machine learning accuracy. *EPJ Quantum Technology*, 11(1):72, 2024.

[13] Matthias C Caro, Elies Gil-Fuster, Johannes Jakob Meyer, Jens Eisert, and Ryan Sweke. Encoding-dependent generalization bounds for parametrized quantum circuits. *Quantum*, 5:582, 2021.

[14] Kaiwen Gui, Alexander M Dalzell, Alessandro Achille, Martin Suchara, and Frederic T Chong. Spacetime-efficient low-depth quantum state preparation with applications. *Quantum*, 8:1257, 2024.

[15] Daniel Malz, Georgios Styliaris, Zhi-Yuan Wei, and J Ignacio Cirac. Preparation of matrix product states with log-depth quantum circuits. *Physical Review Letters*, 132(4):040404, 2024.

[16] Rui Mao, Guojing Tian, and Xiaoming Sun. Toward optimal circuit size for sparse quantum state preparation. *Physical Review A*, 110(3):032439, 2024.

[17] Vaishali Sood and Rishi Pal Chauhan. Towards quantum state preparation with materials science: An analytical review. *International Journal of Quantum Chemistry*, 123(18):e27148, 2023.

[18] Seunghoon Lee, Joonho Lee, Huachen Zhai, Yu Tong, Alexander M Dalzell, Ashutosh Kumar, Phillip Helms, Johnnie Gray, Zhi-Hao Cui, Wenyuan Liu, et al. Evaluating the evidence for exponential quantum advantage in ground-state quantum chemistry. *Nature communications*, 14(1):1952, 2023.

[19] Yudong Cao, Jonathan Romero, Jonathan P Olson, Matthias Degroote, Peter D Johnson, Mária Kieferová, Ian D Kivlichan, Tim Menke, Borja Peropadre, Nicolas PD Sawaya, et al. Quantum chemistry in the age of quantum computing. *Chemical reviews*, 119(19):10856–10915, 2019.

[20] Nicholas J Ward, Ivan Kassal, and Alán Aspuru-Guzik. Preparation of many-body states for quantum simulation. *The Journal of chemical physics*, 130(19), 2009.

[21] IBM. How ibm will build the world’s first large-scale, fault-tolerant quantum computer. <https://www.ibm.com/quantum/blog/large-scale-ftqc>, 2025.

[22] IBM. Quantum roadmap. <https://www.ibm.com/roadmaps/quantum/>, 2025.

[23] Sergey Bravyi, Andrew W Cross, Jay M Gambetta, Dmitri Maslov, Patrick Rall, and Theodore J Yoder. High-threshold and low-overhead fault-tolerant quantum memory. *Nature*, 627(8005):778–782, 2024.

[24] Tanuj Khattar and Craig Gidney. Rise of conditionally clean ancillae for efficient quantum circuit constructions. *Quantum*, 9:1752, 2025.

[25] Avimita Chatterjee, Archisman Ghosh, and Swaroop Ghosh. Quantum prometheus: Defying overhead with recycled ancillas in quantum error correction. In *2025 26th International Symposium on Quality Electronic Design (ISQED)*, pages 1–7. IEEE, 2025.

[26] Pei Yuan and Shengyu Zhang. Optimal (controlled) quantum state preparation and improved unitary synthesis by quantum circuits with any number of ancillary qubits. *Quantum*, 7:956, 2023.

[27] Pei Yuan, Jonathan Allcock, and Shengyu Zhang. Does qubit connectivity impact quantum circuit complexity? *IEEE Transactions on Computer-Aided Design of Integrated Circuits and Systems*, 2023.

[28] Michael A Nielsen and Isaac L Chuang. *Quantum Computation and Quantum Information*. 2000.

[29] Lov Grover and Terry Rudolph. Creating superpositions that correspond to efficiently integrable probability distributions. *arXiv preprint quant-ph/0208112*, 2002.

[30] Mikko Möttönen and Juha J Vartiainen. Decompositions of general quantum gates. *Trends in quantum computing research*, page 149, 2006.

[31] M Mottonen, JJ Vartiainen, V Bergholm, and MM Salomaa. Transformation of quantum states using uniformly controlled rotations. *Quantum Information and Computation*, 5(6):467–473, 2005.

[32] Juha J Vartiainen, Mikko Möttönen, and Martti M Salomaa. Efficient decomposition of quantum gates. *Physical review letters*, 92(17):177902, 2004.

[33] Mikko Möttönen, Juha J Vartiainen, Ville Bergholm, and Martti M Salomaa. Quantum circuits for general multiqubit gates. *Physical review letters*, 93(13):130502, 2004.

[34] Ville Bergholm, Juha J Vartiainen, Mikko Möttönen, and Martti M Salomaa. Quantum circuits with uniformly controlled one-qubit gates. *Physical Review A—Atomic, Molecular, and Optical Physics*, 71(5):052330, 2005.

[35] VV Shende, SS Bullock, and IL Markov. Synthesis of quantum-logic circuits. *IEEE Transactions on Computer-Aided Design of Integrated Circuits and Systems*, 25(6):1000–1010, 2006.

[36] Martin Plesch and Časlav Brukner. Quantum-state preparation with universal gate decompositions. *Physical Review A—Atomic, Molecular, and Optical Physics*, 83(3):032302, 2011.

[37] Raban Iten, Roger Colbeck, Ivan Kukuljan, Jonathan Home, and Matthias Christandl. Quantum circuits for isometries. *Physical Review A*, 93(3):032318, 2016.

[38] Xiao-Ming Zhang, Man-Hong Yung, and Xiao Yuan. Low-depth quantum state preparation. *Physical Review Research*, 3(4):043200, 2021.

[39] Gregory Rosenthal. Query and depth upper bounds for quantum unitaries via grover search. *arXiv preprint arXiv:2111.07992*, 2021.

[40] Xiaoming Sun, Guojing Tian, Shuai Yang, Pei Yuan, and Shengyu Zhang. Asymptotically optimal circuit depth for quantum state preparation and general unitary synthesis. *IEEE Transactions on Computer-Aided Design of Integrated Circuits and Systems*, 42(10):3301–3314, 2023.

[41] Xiao-Ming Zhang, Tongyang Li, and Xiao Yuan. Quantum state preparation with optimal circuit depth: Implementations and applications. *Physical Review Letters*, 129(23):230504, 2022.

[42] Giacomo Belli, Andrea Bersellini, and Michele Amoretti. Quantum State Preparation with Λ -type Operators (qsp-sun). <https://github.com/qslab-unipr/qsp-sun>, 2024.

[43] Giacomo Belli, Andrea Bersellini, and Michele Amoretti. Implementation of an optimally bounded algorithm for quantum state preparation. In *International Conference on Reversible Computation*, pages 37–53. Springer, 2025.

[44] Mikko Mottonen, Juha J Vartiainen, Ville Bergholm, and Martti M Salomaa. Transformation of quantum states using uniformly controlled rotations. *arXiv preprint quant-ph/0407010*, 2004.

[45] Xiaoming Sun, Guojing Tian, Shuai Yang, Pei Yuan, and Shengyu Zhang. Asymptotically optimal circuit depth for quantum state preparation and general unitary synthesis. *arXiv preprint arXiv:2108.06150*, 2021.

[46] Giacomo Belli, Marco Mordacci, and Michele Amoretti. Srbb-based quantum state preparation. In *Proceedings of the 22nd ACM International Conference on Computing Frontiers*, pages 172–175, 2025.

[47] Ville Bergholm, Josh Izaac, Maria Schuld, Christian Gogolin, Shahnawaz Ahmed, Vishnu Ajith, M Sohaib Alam, Guillermo Alonso-Linaje, B AkashNarayanan, Ali Asadi, et al. PennyLane: Automatic differentiation of hybrid quantum-classical computations. *arXiv preprint arXiv:1811.04968*, 2018.

[48] José Alex de Carvalho, Carlos Batista, Tiago de Veras, Israel Araujo, and Adenilton José da Silva. Quantum multiplexer simplification for state preparation. *ACM Transactions on Quantum Computing*, 6(4):1–12, 2025.